Published in final edited form as:
Oncogene. 2008 June 26; 27(28): 3999–4007. doi:10.1038/onc.2008.15.

N-MYC IS A NOVEL REGULATOR OF PI3K–MEDIATED VEGF EXPRESSION IN NEUROBLASTOMA

Junghee Kang[1], **Piotr G. Rychahou**[1], **Titilope A. Ishola**[1], **Joshua M. Mourot**[1], **B. Mark Evers**[1,2], and **Dai H. Chung**[1,2]

1 *Department of Surgery, The University of Texas Medical Branch, Galveston, TX 77555*

2 *Sealy Center for Cancer Cell Biology, The University of Texas Medical Branch, Galveston, TX 77555*

Abstract

Angiogenesis in neuroblastoma (NB) correlates with increased expression of vascular endothelial growth factor (VEGF) and a worse clinical outcome. Other cellular markers, such as Akt activation and *MYCN* amplification, are also associated with poor prognosis in NB; therefore, we sought to determine the role of N-myc in the regulation of the phosphatidylinositol 3-kinase (PI3K)/Akt/VEGF pathway. PI3K inhibition, using small-molecule inhibitors or PTEN adenovirus, led to decreased levels of VEGF mRNA and/or protein by reducing phosphorylation of Akt and mammalian target of rapamycin (mTOR), and attenuating hypoxia-inducible factor 1α (HIF-1α) expression. Moreover, PI3K inhibition decreased levels of N-myc expression in *MYCN*-amplified cells. To further clarify the importance of N-myc as a target of PI3K in VEGF regulation, we inhibited N-myc expression by siRNA transfection. *MYCN* siRNA significantly blocked VEGF secretion, irrespective of serum conditions, in *MYCN*-amplified NB cells; this effect was enhanced when combined with rapamycin, an mTOR inhibitor. Interestingly, in cells with low N-myc expression, *MYCN* siRNA reduction of VEGF secretion was only effective with *MYCN* overexpression or IGF-1 stimulation. Our results show that N-myc plays an important role in the PI3K-mediated VEGF regulation in NB cells. Targeting *MYCN*, as a novel effector of PI3K-mediated angiogenesis, has significant potential for the treatment of highly vascularized, malignant NB.

Keywords

angiogenesis; PI3K/Akt; *MYCN*; VEGF; neuroblastoma

INTRODUCTION

Neuroblastoma (NB) is the most common extracranial solid tumor in infants and children and accounts for 15% of cancer-related mortalities, largely due to metastatic disease progression (Brodeur, 2003; Maris and Matthay, 1999; Schwab *et al.*, 2003). A dismal prognosis for NB significantly correlates with tumor stage, especially since advanced-stage NB remains predominantly refractory to current multimodal therapeutic options (Brodeur, 2003; Maris and Matthay, 1999). Poor prognostic factors in NB include: > 1 year of age at diagnosis, *MYCN* amplification, unfavorable histology, and increased vascularization (Brodeur, 1990; Maris and Matthay, 1999; Seeger *et al.*, 1985). Of these, *MYCN* amplification, occurring in up to 25% of primary tumors, is considered the most important oncogenic marker, strongly correlating to advanced-stage disease and treatment failure (Brodeur *et al.*, 1984; Seeger *et al.*, 1985).

Correspondence: Dai H. Chung, M.D., Department of Surgery, The University of Texas Medical Branch, 301 University Boulevard, Galveston, Texas 77555-0353, Phone: 409-772-2307, Fax: 409-772-4253, E-mail: dhchung@utmb.edu.

Expression of the amplified *MYCN* oncogene is associated with increased proliferation and enhanced malignant potential (Goodman *et al.*, 1997; Pession *et al.*, 1997; Raschella *et al.*, 1991; Zaizen *et al.*, 1993). We and others have recently reported that targeted knockdown of *MYCN* induces growth arrest and apoptosis in NB cells (Kang *et al.*, 2006b; Nara *et al.*, 2007).

Highly vascular in nature, NB displays increased tumor angiogenesis, which is also related to poor patient outcomes (Meitar *et al.*, 1996). Not surprisingly, *MYCN* amplification correlates with enhanced angiogenic capability in human NB tissue biopsies and cell lines (Ribatti *et al.*, 2002). In addition, overexpression of *MYCN* has been shown to downregulate inhibitors of angiogenesis (Fotsis *et al.*, 1999; Hatzi *et al.*, 2000). Vascular endothelial growth factor (VEGF) is an important mediator of vascularization in NB and its expression is associated with unfavorable histology and increased aggressive behavior (Fukuzawa *et al.*, 2002; Langer *et al.*, 2000). Regulation of VEGF expression involves multiple oncogenic pathways including the phosphatidylinositol 3-kinase (PI3K)/Akt pathway. The PI3K/Akt pathway is a potent regulator of angiogenesis in both normal and cancer tissues (Hamada *et al.*, 2005; Hennessy *et al.*, 2005); mammalian target of rapamycin (mTOR) is one of the downstream effectors of this process (Nakamura *et al.*, 2006; Tan *et al.*, 2004). Recently, activated Akt, the critical mediator of PI3K, has been shown to be a prognostic indicator of poor outcome in patients with NB (Opel *et al.*, 2007) and was found to be specifically associated with late-stage and high-grade tumors. Furthermore, PI3K can regulate N-myc protein stabilization in NB cells (Chesler *et al.*, 2006). However, it is unclear whether the PI3K pathway and N-myc collaborate to regulate angiogenesis in NB.

In this study, we demonstrate that PI3K inhibition with chemical inhibitors (i.e. LY294002 or wortmannin) or PTEN adenovirus blocks VEGF expression and secretion. For the first time, we provide evidence that PI3K regulates VEGF via *MYCN*-dependent mechanisms. N-myc represents a critical target for VEGF regulation; therefore, *MYCN* amplification may play an essential role in regulating PI3K-stimulated VEGF levels in NB cells. Importantly, our findings suggest a distinct functional relationship between two major indicators of NB prognosis—N-myc and Akt activation—and their role in directing critical angiogenic pathways.

RESULTS

Inhibition of PI3K decreases NB xenograft growth and angiogenesis *in vivo*

PI3K inhibition has been shown to reduce tumor growth of murine NB (Chesler *et al.*, 2006). To determine the effects of PI3K inhibition on the angiogenic capacity of human NB *in vivo*, we used wortmannin, a selective inhibitor of PI3K that binds to the catalytic subunit p110 (Oikawa and Shimamura, 1996; Powis *et al.*, 1994). Athymic nude mice with established SK-N-SH xenografts were treated with intraperitoneal (i.p.) injections of wortmannin or ethanol vehicle for 23 d. Phosphorylated (p)-Akt was effectively suppressed (p=0.003) while total Akt levels remained constant, verifying the selectivity of wortmannin (Fig. 1C). In fact, the inhibitory effects of wortmannin *in vivo* were observed as early as 0.5 hours following injection (Supplemental Fig. 1). As shown in Fig. 1A, there was a significant reduction in tumor volume by 43% (*left*) and tumor weight by 50% (*right*) in mice treated with wortmannin in comparison to vehicle controls. Since the growth of transplanted tumors largely depends on the angiogenic capacity of the tumor (Kang *et al.*, 2007), we examined tumor angiogenesis by immunohistochemical staining using VEGF and platelet/endothelial cell adhesion molecule-1 (PECAM-1) antibodies. Wortmannin administration decreased VEGF expression and endothelial components of NB xenograft vasculature when compared to controls (Fig. 1B, *left*). A significant decrease in intratumoral microvessel density (IMD), assessed by the quantification of PECAM-1 staining, was observed in tumors from wortmannin-treated group when compared to the control group (100: control group vs. 73.7: wortmannin group) (Fig.

1B, *right*). In addition, VEGF expression was lower in the wortmannin-treated group relative to the control group (p=0.08). PI3K inhibition also decreased circulating plasma VEGF concentrations compared to control levels (Fig. 1D). Collectively, these data show that PI3K blockade affects VEGF expression and arrests growth of established human NB tumors *in vivo*.

PI3K/mTOR pathway regulates VEGF expression and secretion through HIF-1α in NB cells

Since wortmannin treatment decreased VEGF expression in mice bearing NB xenografts, we next wanted to confirm this finding *in vitro*. Treatment with wortmannin or LY294002, another small-molecule PI3K inhibitor, resulted in a significant reduction in the phosphorylation of Akt and mTOR in SK-N-SH, BE(2)-C, JF and LAN-1 cells (Fig. 2A). Additionally, VEGF mRNA expression was significantly decreased by either inhibitor (Fig. 2B). This effect also correlated with a reduction of VEGF secretion into the culture media (Fig. 2C). We further investigated the role of PI3K in NB angiogenesis by specific inhibition of its catalytic subunit p110α with siRNA (sip110α). Compared to the control (siNTC) group, sip110α treatment significantly reduced p110α mRNA and protein levels in all four cell lines (Supplemental Fig. 2B). We also found decreased VEGF secretion in sip110α-transfected cells when compared to siNTC-transfected cells (Supplemental Fig. 2A). Taken together, these results show that PI3K regulates VEGF expression at both the mRNA and protein levels in NB cells.

It has previously been established that activation of PI3K/Akt by growth factors, including insulin-like growth factor (IGF)-1, leads to the phosphorylation of mTOR and induces hypoxia-inducible factor 1α (HIF-1α)-initiated VEGF transcription in NB cells (Beppu *et al.*, 2005; Nakamura *et al.*, 2006). As expected, IGF-1 stimulated phosphorylation of Akt and mTOR and increased HIF-1α expression with concurrent secretion of VEGF into medium in SK-N-SH and BE(2)-C cells; this effect was abrogated by LY294002 (Fig. 3A, B). Rapamycin, the selective inhibitor of mTOR, also downregulated HIF-1α protein levels and inhibited VEGF secretion in JF and LAN-1 cells, but its inhibition was not significant in SK-N-SH and BE(2)-C cells (Fig. 3C). Interestingly, rapamycin significantly inhibited IGF-1-stimulated VEGF secretion in all four NB cell lines under IGF-1 stimulation. These data suggest that PI3K regulates other angiogenic mechanisms in NB cells, in addition to the mTOR-dependent pathway.

PI3K inhibition regulates IGF-1 mediated N-myc and VEGF expression

Recently, PI3K inhibition has been shown to induce N-myc degradation (Chesler *et al.*, 2006). N-myc overexpression, an important determinant of NB prognosis, is associated with vascularization in NB (Meitar *et al.*, 1996; Ribatti *et al.*, 2002). Therefore, we next wanted to explore whether PI3K interacts with N-myc to regulate angiogenic pathways. In order to confirm whether PI3K regulates N-myc, *MYCN*-amplified BE(2)-C cells were serum-starved, treated with IGF-1 and/or LY294002, and the levels of N-myc protein were assessed. There was an upregulation of N-myc expression after IGF-1 stimulation in BE(2)-C cells. LY294002 treatment reduced N-myc expression in both the absence and presence of IGF-1 (Fig. 4A). To further confirm the mechanism involved in this process, we transiently overexpressed PTEN, the negative regulator of the PI3K/Akt pathway, using adenovirus infection in BE(2)-C cells. IGF-1-stimulated N-myc expression was significantly inhibited in PTEN infected cells when compared to control adenovirus infected cells (Fig. 4B; *left*). Additionally, VEGF secretion was decreased in both unstimulated and IGF-1-stimulated PTEN overexpressing BE(2)-C cells (Fig. 4B; *right*).

N-myc expression regulates VEGF secretion in NB cells

We then wanted to investigate whether specific inhibition of N-myc could regulate VEGF expression. BE(2)-C and IMR-32 cells were transfected with siRNA against *MYCN* (siMYCN)

for 72 h and VEGF secretion into the medium was assessed. As shown in Fig. 4C, siMYCN significantly decreased VEGF expression along with N-myc expression in *MYCN*-amplified BE(2)-C and IMR-32 cells. In contrast, *MYCN*-unamplified SK-N-SH did not show any difference in VEGF secretion after transfection when compared to siNTC-transfected cells; N-myc expression was also undetectable (Fig. 4C). In order to confirm the specificity of the siRNA, we assessed the effects of two separate single sequences (siMYCN1 and siMYCN2); both were able to establish sufficient knockdown of N-myc (Supplemental Fig. 3).

For the purpose of verifying the role of N-myc, we transfected *MYCN*-unamplified SK-N-SH cells with a *MYCN* expression vector, which strongly upregulated N-myc mRNA and protein expression (Fig. 5A, *bottom*). This increase in N-myc expression caused a significant increase in VEGF secretion, in contrast to cells transfected with the control vector (Fig. 5A, *top*). We further confirmed that these effects were dependent on N-myc expression by using siRNA to silence *MYCN* expression in SK-N-SH cells transfected with the *MYCN* vector (Fig. 5B, *top*). *MYCN* silencing in SK-N-SH-MYCN cells reduced VEGF secretion, in comparison to siNTC-transfected cells. We also noted effective N-myc knockdown by QRT-PCR and Western blot analysis (Fig. 5B, *bottom*). Taken together, these findings indicate that the regulation of VEGF in NB cells is, in part, dependent on the expression of N-myc.

MYCN silencing attenuates VEGF secretion, and enhances rapamycin-mediated inhibition of VEGF secretion

To assess the effect of N-myc downregulation on VEGF expression in a setting of PI3K activation, we treated *MYCN*-amplified BE(2)-C, JF, LAN-1 and *MYCN*-unamplified SK-N-SH cells with siMYCN in the presence or absence of IGF-1. siMYCN decreased VEGF secretion in high-N-myc expressing cell lines, whereas this downregulation occurred only upon IGF-1 stimulation in low-N-myc expressing SK-N-SH cells (Fig. 6A). Unlike LY294002 and PTEN (Fig. 4), rapamycin did not inhibit N-myc expression (Fig. 6B); however, the inhibitory effects of siMYCN on VEGF secretion were enhanced when combined with rapamycin treatment in *MYCN*-amplified cells (Fig. 6B). Treatment with siMYCN facilitated rapamycin inhibition of IGF-1 stimulated VEGF secretion to a lesser extent in SK-N-SH cells. These data further confirm the findings that N-myc is a downstream target of PI3K, in the context of VEGF regulation, and may act in conjunction with mTOR activation.

DISCUSSION

Aggressive progression of NB significantly correlates with the degree of tumor vascularity (Meitar *et al.*, 1996; Ribatti *et al.*, 2002); and in particular, this progression is marked by increased levels of the angiogenic marker VEGF (Fukuzawa *et al.*, 2002). The PI3K/Akt pathway is a crucial regulator of angiogenesis (Hamada *et al.*, 2005) and increased activity has been determined to be a portent of poor prognosis in NB (Opel *et al.*, 2007). Malignant, high-grade tumors are frequently characterized by amplification of the *MYCN* oncogene (Meitar *et al.*, 1996; Ribatti *et al.*, 2002), which is present in 30% of advanced-stage tumors (Brodeur, 2003). In this study, we sought to evaluate the importance of N-myc in PI3K-mediated VEGF expression in NB. We identified strong expression of VEGF protein in control tumors *in vivo* and detected systemic levels of VEGF in nude mice, in contrast to mice treated with wortmannin. The inhibition of PI3K-mediated VEGF expression was further confirmed *in vitro*, further verifying the essential role of the PI3K pathway in regulating angiogenesis in NB. We also found that PI3K activation increased N-myc protein levels; this PI3K-induced N-myc stabilization was associated with an increase in VEGF secretion. Our findings strongly suggest that PI3K/Akt activation and *MYCN*, two factors associated with poor outcome in NB, contribute to the vascularity of NB and, therefore, may be ideal targets for NB treatment strategies.

PI3K/Akt stimulation of angiogenesis is mediated, in part, by mTOR and HIF-1α (Fukuda *et al.*, 2002; Jiang *et al.*, 2001; Laughner *et al.*, 2001; Marimpietri *et al.*, 2005; Nakamura *et al.*, 2006; Tan *et al.*, 2004). Our results further establish that PI3K/Akt acts through mTOR and HIF-1α to regulate VEGF in NB. However, we noted that in all of our cell lines, rapamycin-induced inhibition of VEGF was significant only in the presence of IGF-1. Recently, Kurmasheva et al. postulated that VEGF expression in unstimulated NB cells depends on PI3K/Akt-driven signaling that most likely bypasses mTOR (Kurmasheva *et al.*, 2007). They observed that HIF-1α and VEGF expression was strongly decreased with an Akt inhibitor, but was inadequately affected by rapamycin treatment in standard (10%) serum conditions. Furthermore, in another study, Akt siRNA, but not rapamycin or mTOR siRNA, inhibited HIF-1α expression in glioblastoma and prostate cancer cells maintained in 10% serum conditions (Pore *et al.*, 2006). However, in that particular study, rapamycin inhibition HIF1α could be achieved in the presence of lower serum concentrations. This corresponds with our findings in some of our NB cells, since the rapamycin studies were carried out in serum-free conditions. The mechanism is still unclear; however, it is likely that mTOR contributes more significantly to PI3K-mediated angiogenesis in the context of nutrient depletion. Furthermore, PI3K stimulation by growth factors, such as IGF-1, may enhance the sensitivity of the mTOR/VEGF pathway to rapamycin.

Our study further identifies N-myc as a key mediator of PI3K-regulated VEGF expression in NB. PI3K activation was first shown to regulate N-myc in cerebellar neuronal precursors by stabilizing N-myc steady-state levels through GSK-3β inhibition (Kenney *et al.*, 2004). This observation was also noted in NB cells where LY294002 destabilized N-myc protein in a GSK-3β-dependent manner (Chesler *et al.*, 2006). Our results, using PTEN overexpression or LY294002, corroborate the significance of PI3K regulation on N-myc expression. Moreover, simultaneous inhibition of N-myc and mTOR resulted in cooperative downregulation of VEGF secretion, suggesting that PI3K stimulation of N-myc expression and mTOR activation may be independent of each other. In fact, we observed that rapamycin had no effect on IGF-1-induced N-myc levels in NB cells; this corroborates work reported by Misawa et al. (Misawa *et al.*, 2003). Therefore, we have identified, for the first time, that N-myc is a novel effector of PI3K-mediated VEGF expression in NB and may operate through pathways distinct from mTOR (Fig. 7). If these pathways are indeed separate, we postulate that under normal or nutrient-depleted growth conditions, PI3K can regulate N-myc to induce VEGF expression; however, it is possible that PI3K may subsequently activate mTOR as a failsafe for angiogenic permanence in the absence of adequate nourishment.

Although N-myc expression has been shown to downregulate inhibitors of angiogenesis (Hatzi *et al.*, 2000), its function in VEGF-mediated angiogenesis is relatively unknown. On the other hand, C-myc, another member of the *MYC* oncogene family, is an important regulator of angiogenesis in developmental and tumor tissues, and is positively associated with VEGF expression (Baudino *et al.*, 2002; Dews *et al.*, 2006; von Rahden *et al.*, 2006). Here, we report that *MYCN* silencing effectively blocked VEGF expression in *MYCN*-amplified cell lines, regardless of serum conditions. Whereas, in low-N-myc expressing cells, *MYCN* knockdown could only attenuate VEGF levels subsequent to *MYCN* overexpression or IGF-1 stimulation. Therefore, N-myc functions as a crucial regulator of VEGF in an expression-dependent manner, indicating another role for N-myc in NB angiogenesis. Moreover, it appears that mechanisms that increase N-myc stability, such as PI3K activation, are also susceptible to inhibitors of N-myc expression.

In conclusion, our findings suggest that predictors of an unfavorable prognosis in NB, N-myc and PI3K/Akt activation, may have more than a coincidental relationship and may in fact be interdependent. Further studies will be necessary in order to delineate the molecular mechanisms of PI3K/N-myc/VEGF regulation of angiogenesis. These results are of clinical

relevance to NB because, as heterogeneous tumors, multiple therapeutic targets will be required to effectively deter tumor progression and improve the survival rate in advanced, highly vascularized NB.

MATERIALS AND METHODS

Reagents

Antibodies against VEGF and horseradish peroxidase (HRP)-conjugated secondary antibodies were purchased from Santa Cruz Biotechnology, Inc. (Santa Cruz Biotechnology, Inc., CA). PECAM-1 and HIF-1α antibodies were from BD Biosciences (San Jose, CA). LY294002, rapamycin, and antibodies against p-Akt (Ser 473), Akt, p110α, p-mTOR (Ser 2448) and mTOR were obtained from Cell Signaling Technology (Beverly, MA). N-myc antibody was from EMD Chemicals, Inc. (San Diego, CA). siRNAs (siMYCN and siNTC) were from Dharmacon, Inc. (Lafayette, CO). Adenoviral vectors expressing PTEN (Ad-PTEN) and luciferase (Ad-Luc) under the control of a cytomegalovirus promoter were obtained from Vector Biolabs (Philadelphia, PA). *MYCN* (pCMV6-XL4-MYCN) and control (pCMV6-XL4) vectors were purchased from Origene (Rockville, MD). All cell culture related products were from Mediatech, Inc. (Herndon, VA), unless otherwise specified. RNAqueous kit was obtained from Ambion, Inc. (Austin, TX). Lipofectamine 2000 and Hanks Balanced Salt Solution (HBSS) were from Invitrogen (Rockville, MD). Reagents for immunohistochemistry were purchased from either Dako Corporation (Carpinteria, CA) or Richard-Allan Scientific (Kalamazoo, MI). Recombinant human IGF-1 and VEGF enzyme-linked immunosorbent assay (ELISA) kit were from R&D Systems, Inc. (Minneapolis, MN).

Cell culture, siRNA transfection, and adenovirus infection

Human NB cell lines, SK-N-SH, BE(2)-C and IMR-32 were purchased from American Type Culture Collection (Manassas, VA). JF, a primary NB cell line, was a gift from Dr. Jason M. Shohet (Baylor College of Medicine, Houston, TX) and LAN-1 was a gift from Dr. Robert C. Seeger (University of Southern California, Los Angeles, CA). Cells were grown in RPMI 1640 or EMEM medium with 10% fetal bovine serum (FBS) and maintained at 37°C in a humidified atmosphere of 95% air and 5% CO_2. For siRNA or plasmid transfection assay, 6–9 × 10^6 cells/400 μl or 2–5 × 10^5 cells/well were transfected with siMYCN or siNTC, *MYCN* or control vector by Lipofectamine 2000 as previously described (Kang *et al.*, 2006b). The sequences for siMYCN were GAAGAAAUCGACGUGGUCAUU(5′-PUGACCACGUCGAUUUCUUCUU), GAGAGGACACCCUGAGCGAUU(5′-PUCGCUCAGGGUGUCCUCUCUU), GAACCCAGACCUCGAGUUUUU(5′-PAAACUCGAGGUCUGGGUUCUU), and GGACAGUGAGCGUCGCAGAUU(5′-PUCUGCGACGCUCACUGUCCUU). Cells were harvested for quantitative RT-PCR (QRT-PCR), VEGF ELISA or Western blot at indicated times. For IGF-1 studies, the attached cells were serum-starved for 24 h and treated with IGF-1 alone or in combination with inhibitors. The concentrations of IGF-1, LY294002, wortmannin, rapamycin, and dimethylsulfoxide (DMSO) were 100 nM, 20 μM, 500nM, 50 nM, and 0.1%, respectively. Adenovirus infection was performed according to the company's instructions. Briefly, recombinant Ad-PTEN or Ad-Luc was diluted in cell culture media containing 2% FBS and added to subconfluent cells in 6-well plates for 6 h at a multiplicity of infection of 40. The medium was then replaced and the cells were incubated for 18 h.

RNA isolation and real time QRT-PCR

Total cellular RNA extraction and real time QRT-PCR were carried out as previously described (Kang *et al.*, 2007; Kang *et al.*, 2006b). Briefly, we used applied biosystems (Foster City, CA) assays-on-demand 20x assay mix of primers and TaqMan MGB probes (FAM™ dye-labeled) for the target genes, human *VEGF* (NM_003376, Hs00173626_m1), *MYCN* (NM 005378,

Hs00232074_m1) and pre-developed 18S rRNA (VIC™-dye labeled probe) TaqMan® assay reagent (P/N 4319413E) for endogenous control. For relative quantitation of gene expression, separate tubes (singleplex) one-step RT-PCR was performed with 80ng RNA for both target genes and endogenous control. The reagent we used was TaqMan one-step RT-PCR master mix reagent kit (P/N 4309169). The cycling parameters for one-step RT-PCR was: reverse transcription 48°C for 30 min, AmpliTaq activation 95°C for 10 min, denaturation 95°C for 15 sec and annealing/extension 60°C for 1 min (repeat 40 times) on ABI7000. Duplicate CT values were analyzed in Microsoft Excel using the comparative CT (ΔΔCT) method as described by the manufacturer (Applied Biosystems, Foster City, CA). The amount of target (2-ΔΔCT) was obtained by normalization to an endogenous reference (18s) and relative to a calibrator (one of the experimental samples).

Xenograft studies

Male athymic nude mice (4–6 weeks old) were obtained from Harlan Sprague Dawley (Indianapolis, IN). All studies were approved by the Institutional Animal Care and Use Committee at the University of Texas Medical Branch.

Mice were anesthetized and xenografts were established by subcutaneous injection of 10×10^6 SK-N-SH cells/100 μl HBSS into the bilateral flanks using a 26-gauge needle. After 34 days, the mice were randomized into two experimental groups (n=5/group): control (vehicle; 5% ethanol in saline) and wortmannin (1.5 mg/kg/day; 5% ethanol in saline). All injections were administered i.p. q 12 h. Tumor growth was assessed bi-weekly by measuring the two greatest perpendicular tumor dimensions with vernier calipers (Mitutoyo, Tokyo, Japan) and body weights were recorded weekly. The tumor volumes were calculated as follows: tumor volume (mm^3) = [tumor length (mm) × tumor width $(mm)^2$]/2. At sacrifice, tumors and organs were excised, weighed, and snap frozen in liquid nitrogen for storage at −80°C for further assays; plasma was collected for ELISA.

Immunoblotting

Whole-cell lysates or tissues were prepared as previously described (Kang *et al.*, 2007; Kang *et al.*, 2006a). Briefly, total protein was resolved on Bis-Tris gels and electrophoretically transferred to PVDF membranes. Target proteins were detected by using rabbit or mouse anti-human antibodies (1:200–1000 dilutions). The membranes were washed and incubated with secondary antibodies (1:5000 dilution) conjugated with HRP. Immune complexes were visualized using the enhanced chemiluminescence system. Equal protein loading was confirmed by blotting the same membrane with β-actin antibody.

Immunohistochemistry

For VEGF staining, xenografts were fixed in formalin overnight and embedded in paraffin wax. Tumor sections (5 μm) were mounted on glass slides and staining performed as previously described (Kang *et al.*, 2007). For PECAM-1 staining, frozen NB xenografts were embedded in O.C.T. compound, mounted (5 μm) on slides, fixed by immersion in cold acetone for 2 min at −20°C, and then air dried. Slides were washed with PBS, incubated in 3% H_2O_2 solution in methanol for 10 min and then washed with PBS. Sections were incubated with primary antibody (1:100 dilution) overnight at 4°C, washed and incubated with biotinylated anti-Ig secondary antibody (1:50) followed by incubation with streptravidin-HRP for 30min at RT. Sections were developed with DAB reagent and the reaction was terminated by immersing slides in dH_2O. Slides were then dehydrated, mounted and left to dry.

VEGF ELISA

For *in vitro* studies, the supernatant from cultured cells was collected at the indicated time points. For *in vivo* studies, blood was collected with EDTA to prevent coagulation, centrifuged at 2×10^3 rpm at RT for 15 min, and plasma stored at −80°C. For assay, samples were thawed, centrifuged, and VEGF levels were measured using human VEGF ELISA kit according to the manufacturer's instructions. All experiments were performed on at least two separate occasions.

Statistical analyses

Tumor size and body weight were analyzed using analysis of variance (ANOVA) for a two-factor experiment with repeated measures on time in SK-N-SH *in vivo* experiments. All effects were assessed at the 0.05 level of significance and all interactions of the effects were assessed at the 0.15 level of significance as the experiment-wise error rates. Fisher's least significant difference procedure was used for multiple comparisons with 0.005 as the comparison-wise error rate. Data analysis was conducted using PROC MIXED with LSMEANS option and Satterthwaite approximation for the denominator degrees of freedom in SAS®, Release 9.1 (SAS Institute Inc., Cary, NC). IMD was captured using Image J software (NIH) and quantitated by analyzing 18 random fields from all samples (n=5 mice per group). Image J was also used to perform the densitometric analysis of *in vivo* protein expression from immunoblots. For tumor mass and *in vitro* studies, statistical analyses were performed using one-way ANOVA for comparisons between the treatment groups. A p value <0.05 was considered significant.

Supplementary Material

Refer to Web version on PubMed Central for supplementary material.

Acknowledgements

This work was supported by grants RO1 DK61470, RO1 DK48498, RO1 CA104748 and PO1 DK35608 from the National Institutes of Health.

The authors thank Dr. Mark R. Hellmich for helpful advice on PECAM-1 experiments, Karen K. Martin for manuscript preparation and Tatsuo Uchida for statistical analysis.

References

Baudino TA, McKay C, Pendeville–Samain H, Nilsson JA, Maclean KH, White EL, et al. c–Myc is essential for vasculogenesis and angiogenesis during development and tumor progression. Genes Dev 2002;16:2530–2543. [PubMed: 12368264]

Beppu K, Nakamura K, Linehan WM, Rapisarda A, Thiele CJ. Topotecan blocks hypoxia–inducible factor–1alpha and vascular endothelial growth factor expression induced by insulin–like growth factor–I in neuroblastoma cells. Cancer Res 2005;65:4775–4781. [PubMed: 15930297]

Brodeur GM. Neuroblastoma—clinical applications of molecular parameters. Brain Pathol 1990;1:47–54. [PubMed: 1669693]

Brodeur GM. Neuroblastoma: biological insights into a clinical enigma. Nat Rev Cancer 2003;3:203–216. [PubMed: 12612655]

Brodeur GM, Seeger RC, Schwab M, Varmus HE, Bishop JM. Amplification of N–myc in untreated human neuroblastomas correlates with advanced disease stage. Science 1984;224:1121–1124. [PubMed: 6719137]

Chesler L, Schlieve C, Goldenberg DD, Kenney A, Kim G, McMillan A, et al. Inhibition of Phosphatidylinositol 3–Kinase Destabilizes Mycn Protein and Blocks Malignant Progression in Neuroblastoma. Cancer Res 2006;66:8139–8146. [PubMed: 16912192]

Dews M, Homayouni A, Yu D, Murphy D, Sevignani C, Wentzel E, et al. Augmentation of tumor angiogenesis by a Myc–activated microRNA cluster. Nat Genet 2006;38:1060–1065. [PubMed: 16878133]

Fotsis T, Breit S, Lutz W, Rossler J, Hatzi E, Schwab M, et al. Down–regulation of endothelial cell growth inhibitors by enhanced MYCN oncogene expression in human neuroblastoma cells. Eur J Biochem 1999;263:757–764. [PubMed: 10469139]

Fukuda R, Hirota K, Fan F, Jung YD, Ellis LM, Semenza GL. Insulin–like growth factor 1 induces hypoxia–inducible factor 1–mediated vascular endothelial growth factor expression, which is dependent on MAP kinase and phosphatidylinositol 3–kinase signaling in colon cancer cells. J Biol Chem 2002;277:38205–38211. [PubMed: 12149254]

Fukuzawa M, Sugiura H, Koshinaga T, Ikeda T, Hagiwara N, Sawada T. Expression of vascular endothelial growth factor and its receptor Flk–1 in human neuroblastoma using in situ hybridization. J Pediatr Surg 2002;37:1747–1750. [PubMed: 12483647]

Goodman LA, Liu BC, Thiele CJ, Schmidt ML, Cohn SL, Yamashiro JM, et al. Modulation of N–myc expression alters the invasiveness of neuroblastoma. Clin Exp Metastasis 1997;15:130–139. [PubMed: 9062389]

Hamada K, Sasaki T, Koni PA, Natsui M, Kishimoto H, Sasaki J, et al. The PTEN/PI3K pathway governs normal vascular development and tumor angiogenesis. Genes Dev 2005;19:2054–2065. [PubMed: 16107612]

Hatzi E, Breit S, Zoephel A, Ashman K, Tontsch U, Ahorn H, et al. MYCN oncogene and angiogenesis: down–regulation of endothelial growth inhibitors in human neuroblastoma cells. Purification, structural, and functional characterization. Adv Exp Med Biol 2000;476:239–248. [PubMed: 10949669]

Hennessy BT, Smith DL, Ram PT, Lu Y, Mills GB. Exploiting the PI3K/AKT pathway for cancer drug discovery. Nat Rev Drug Discov 2005;4:988–1004. [PubMed: 16341064]

Jiang BH, Jiang G, Zheng JZ, Lu Z, Hunter T, Vogt PK. Phosphatidylinositol 3–kinase signaling controls levels of hypoxia–inducible factor 1. Cell Growth Differ 2001;12:363–369. [PubMed: 11457733]

Kang J, Ishola TA, Baregamian N, Mourot JM, Rychahou PG, Evers BM, et al. Bombesin induces angiogenesis and neuroblastoma growth. Cancer Lett 2007;253:273–281. [PubMed: 17383815]

Kang J, Kamal A, Burrows FJ, Evers BM, Chung DH. Inhibition of neuroblastoma xenograft growth by Hsp90 inhibitors. Anticancer Res 2006a;26:1903–1908. [PubMed: 16827123]

Kang JH, Rychahou PG, Ishola TA, Qiao J, Evers BM, Chung DH. MYCN silencing induces differentiation and apoptosis in human neuroblastoma cells. Biochem Biophys Res Commun 2006b; 351:192–197. [PubMed: 17055458]

Kenney AM, Widlund HR, Rowitch DH. Hedgehog and PI–3 kinase signaling converge on Nmyc1 to promote cell cycle progression in cerebellar neuronal precursors. Development 2004;131:217–228. [PubMed: 14660435]

Kurmasheva RT, Harwood FC, Houghton PJ. Differential regulation of vascular endothelial growth factor by Akt and mammalian target of rapamycin inhibitors in cell lines derived from childhood solid tumors. Mol Cancer Ther 2007;6:1620–1628. [PubMed: 17483438]

Langer I, Vertongen P, Perret J, Fontaine J, Atassi G, Robberecht P. Expression of vascular endothelial growth factor (VEGF) and VEGF receptors in human neuroblastomas. Med Pediatr Oncol 2000;34:386–393. [PubMed: 10842244]

Laughner E, Taghavi P, Chiles K, Mahon PC, Semenza GL. HER2 (neu) signaling increases the rate of hypoxia–inducible factor 1alpha (HIF–1alpha) synthesis: novel mechanism for HIF–1–mediated vascular endothelial growth factor expression. Mol Cell Biol 2001;21:3995–4004. [PubMed: 11359907]

Marimpietri D, Nico B, Vacca A, Mangieri D, Catarsi P, Ponzoni M, et al. Synergistic inhibition of human neuroblastoma–related angiogenesis by vinblastine and rapamycin. Oncogene 2005;24:6785–6795. [PubMed: 16007159]

Maris JM, Matthay KK. Molecular Biology of Neuroblastoma. J Clin Oncol 1999;17:2264–2279. [PubMed: 10561284]

Meitar D, Crawford SE, Rademaker AW, Cohn SL. Tumor angiogenesis correlates with metastatic disease, N–myc amplification, and poor outcome in human neuroblastoma. Journal of Clinical Oncology 1996;14:405–414. [PubMed: 8636750]

Misawa A, Hosoi H, Tsuchiya K, Sugimoto T. Rapamycin inhibits proliferation of human neuroblastoma cells without suppression of MycN. Int J Cancer 2003;104:233–237. [PubMed: 12569580]

Nakamura K, Martin KC, Jackson JK, Beppu K, Woo C-W, Thiele CJ. Brain–Derived Neurotrophic Factor Activation of TrkB Induces Vascular Endothelial Growth Factor Expression via Hypoxia–Inducible Factor–1{alpha} in Neuroblastoma Cells. Cancer Res 2006;66:4249–4255. [PubMed: 16618748]

Nara K, Kusafuka T, Yoneda A, Oue T, Sangkhathat S, Fukuzawa M. Silencing of MYCN by RNA interference induces growth inhibition, apoptotic activity and cell differentiation in a neuroblastoma cell line with MYCN amplification. Int J Oncol 2007;30:1189–1196. [PubMed: 17390021]

Oikawa T, Shimamura M. Potent inhibition of angiogenesis by wortmannin, a fungal metabolite. Eur J Pharmacol 1996;318:93–96. [PubMed: 9007518]

Opel D, Poremba C, Simon T, Debatin KM, Fulda S. Activation of Akt predicts poor outcome in neuroblastoma. Cancer Res 2007;67:735–745. [PubMed: 17234785]

Pession A, Trere D, Perri P, Rondelli R, Montanaro L, Mantovani W, et al. N–myc amplification and cell proliferation rate in human neuroblastoma. J Pathol 1997;183:339–344. [PubMed: 9422991]

Pore N, Jiang Z, Shu HK, Bernhard E, Kao GD, Maity A. Akt1 activation can augment hypoxia–inducible factor–1alpha expression by increasing protein translation through a mammalian target of rapamycin–independent pathway. Mol Cancer Res 2006;4:471–479. [PubMed: 16849522]

Powis G, Bonjouklian R, Berggren MM, Gallegos A, Abraham R, Ashendel C, et al. Wortmannin, a potent and selective inhibitor of phosphatidylinositol–3–kinase. Cancer Res 1994;54:2419–2423. [PubMed: 8162590]

Raschella G, Negroni A, Giubilei C, Romeo A, Ferrari S, Castello MA, et al. Transcription of N–myc and proliferation–related genes is linked in human neuroblastoma. Cancer Lett 1991;56:45–51. [PubMed: 2004353]

Ribatti D, Raffaghello L, Pastorino F, Nico B, Brignole C, Vacca A, et al. In vivo angiogenic activity of neuroblastoma correlates with MYCN oncogene overexpression. Int J Cancer 2002;102:351–354. [PubMed: 12402304]

Schwab M, Westermann F, Hero B, Berthold F. Neuroblastoma: biology and molecular and chromosomal pathology. The Lancet Oncology 2003;4:472–480. [PubMed: 12901961]

Seeger RC, Brodeur GM, Sather H, Dalton A, Siegel SE, Wong KY, et al. Association of multiple copies of the N–myc oncogene with rapid progression of neuroblastomas. N Engl J Med 1985;313:1111–1116. [PubMed: 4047115]

Tan C, Cruet–Hennequart S, Troussard A, Fazli L, Costello P, Sutton K, et al. Regulation of tumor angiogenesis by integrin–linked kinase (ILK). Cancer Cell 2004;5:79–90. [PubMed: 14749128]

von Rahden BH, Stein HJ, Puhringer–Oppermann F, Sarbia M. c–myc amplification is frequent in esophageal adenocarcinoma and correlated with the upregulation of VEGF–A expression. Neoplasia 2006;8:702–707. [PubMed: 16984727]

Zaizen Y, Taniguchi S, Noguchi S, Suita S. The effect of N–myc amplification and expression on invasiveness of neuroblastoma cells. J Pediatr Surg 1993;28:766–769. [PubMed: 8331499]

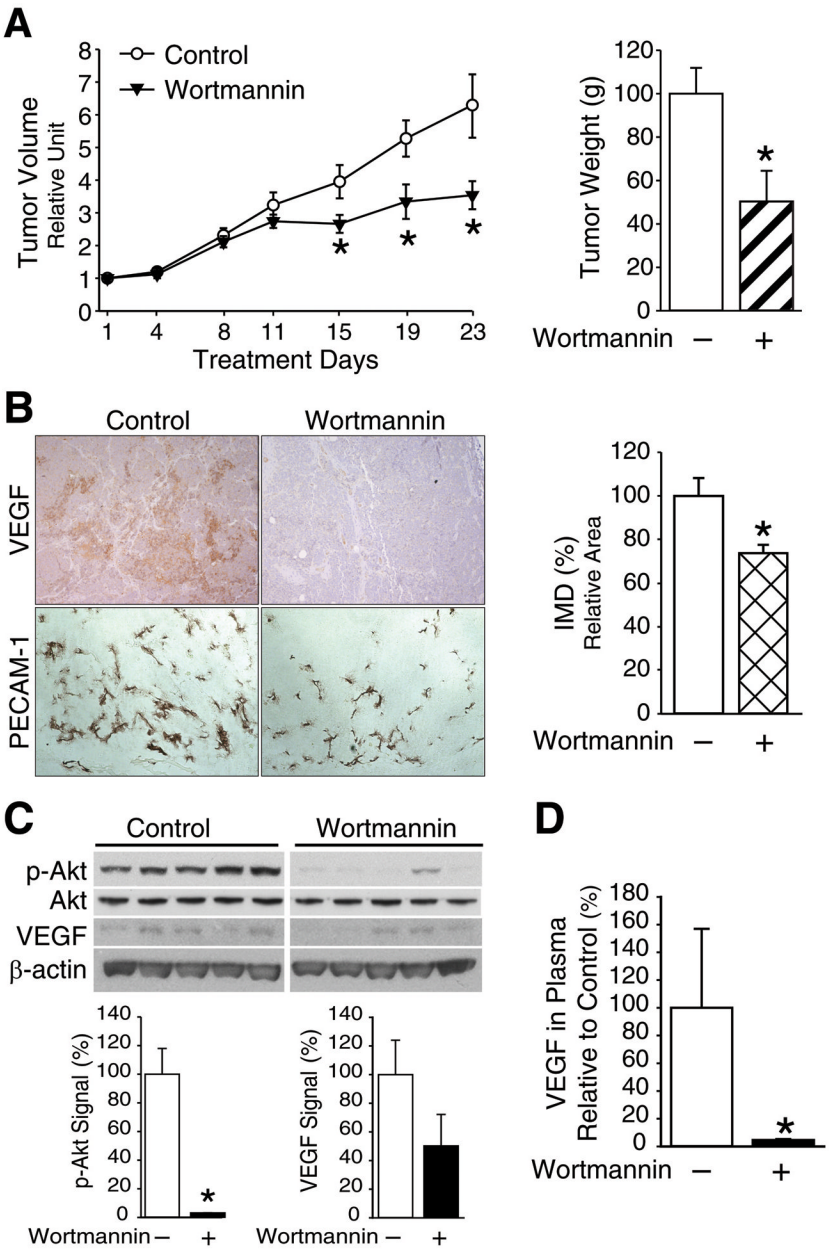

Figure 1. Wortmannin attenuates NB angiogenesis *in vivo*

A. Tumor volumes of subscapular SK-N-SH xenografts in mice treated with vehicle or wortmannin (n=5/group; *left*). Tumor weights of resected tumors at sacrifice (*right*). Data represent mean ± SEM; * p <0.05 vs. control. Relative unit represents the fold change compared to the control group on day 1. **B.** Representative microphotographs of VEGF and PECAM-1 expression. SK-N-SH xenografts from vehicle- or wortmannin-treated mice stained with anti-human VEGF antibody or PECAM-1 antibody (brown); magnification 100X, 200X, respectively (*left*). IMD was assessed by quantifying endothelial cells, using PECAM-1 stained sections (mean ± SEM; * p <0.05 vs. control; *right*). **C.** Western blot analysis of p-Akt, total Akt and VEGF expression in tumor samples treated with vehicle or wortmannin (n=5/group). β-actin was used for loading control; * p <0.05 vs. control. **D.** Plasma concentration of VEGF in control (vehicle) and wortmannin-treated mice (n=5/group; * p <0.05 vs. control).

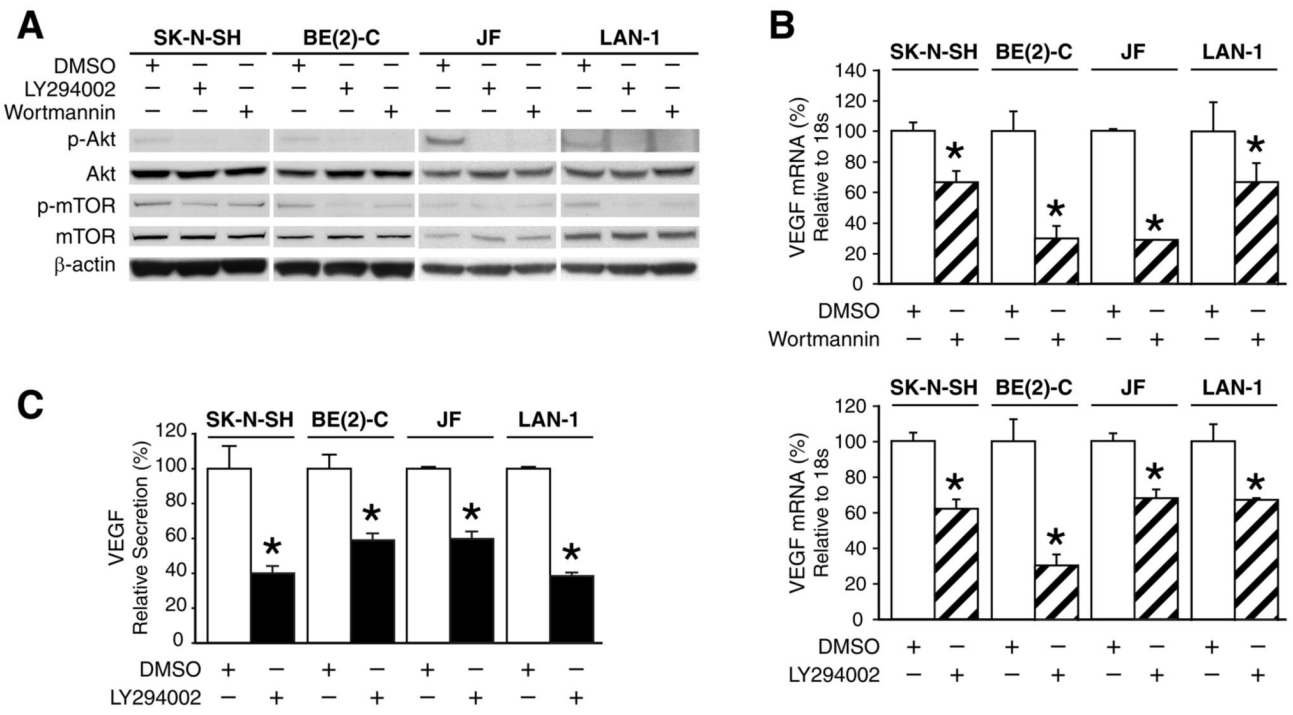

Figure 2. PI3K inhibition reduces VEGF expression in NB cells

A. Subconfluent SK-N-SH, BE(2)-C, JF and LAN-1cells were treated with LY294002, wortmannin or DMSO (control) for 4 h and protein lysates were probed with p-Akt, Akt, p-mTOR and mTOR antibodies. **B.** The cells were treated with wortmannin (*top*) or LY294002 (*bottom*) for 16 h and RNA was isolated and analyzed for VEGF mRNA expression by QRT-PCR. **C.** The cells were treated with LY294002 for 12–16 h and the conditioned medium was analyzed for VEGF secretion. Data represent mean ± SEM; * $p < 0.05$ vs. control.

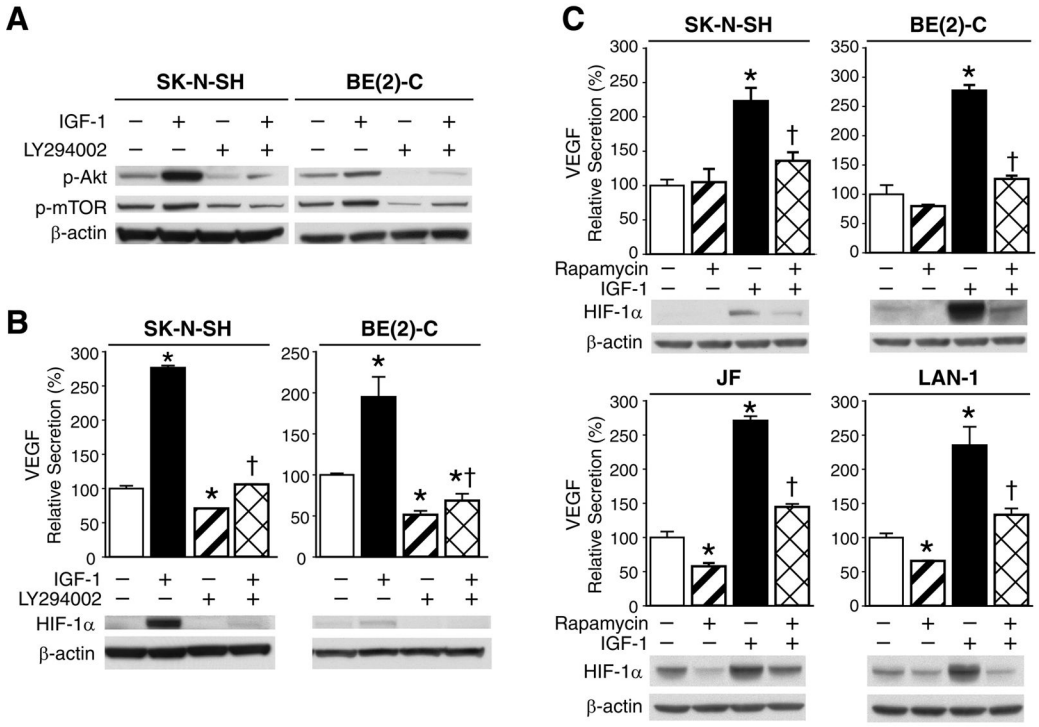

Figure 3. PI3K and mTOR regulate VEGF secretion through HIF-1α

A. Serum-starved subconfluent SK-N-SH and BE(2)-C cells were treated with LY294002 in the absence or presence of IGF-1 for 6 h. Protein lysates were immunoblotted with p-Akt and p-mTOR antibodies. **B.** Serum-starved subconfluent SK-N-SH and BE(2)-C cells were treated with LY294002 in the absence or presence of IGF-1 for 20 h. Conditioned medium was analyzed for VEGF secretion (*top)* and protein lysates were immunoblotted with HIF-1α antibody (*bottom)*. **C.** Serum-starved BE(2)-C, JF, LAN-1 and SK-N-SH cells were treated with rapamycin in the absence or presence of IGF-1 for 18–20 h. Conditioned medium was analyzed for VEGF secretion (*top*) and protein lysates were immunoblotted with HIF-1α antibody (*bottom*). Data represent mean ± SEM; * $p < 0.05$ vs. control, † $p < 0.05$ vs. IGF-1 treated group.

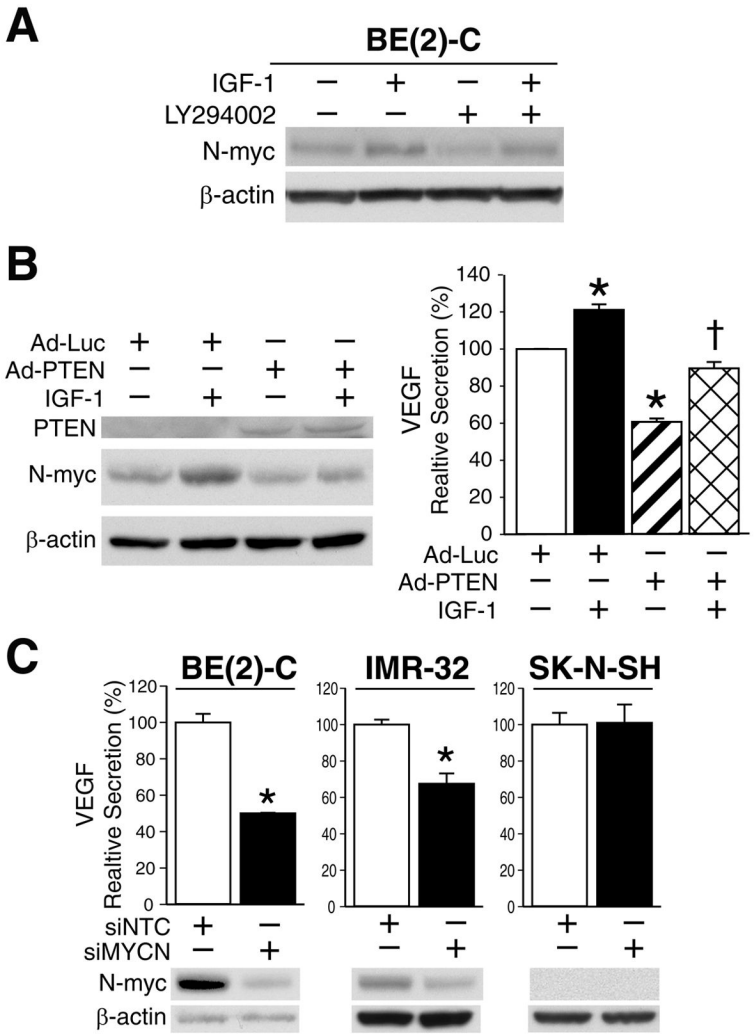

Figure 4. N-myc is regulated by PI3K and N-myc knockdown decreases VEGF expression

A. Serum-starved subconfluent BE(2)-C cells were treated with LY294002 in the absence or presence of IGF-1 for 6 h. Protein lysates were immunoblotted with N-myc antibody. **B.** *MYCN*-amplified BE(2)-C cells were infected with PTEN adenovirus and serum starved for 24 h followed by IGF-1 treatment for 16 h. Protein lysates were probed with PTEN or N-myc antibody (*left*). Conditioned medium was analyzed for VEGF secretion (*right*). **C.** BE(2)-C, IMR-32, and SK-N-SH human NB cell lines were transfected with siMYCN or siNTC for 72 h and the conditioned medium was analyzed for VEGF secretion (*top*). N-myc expression from protein lysates after siMYCN transfection (*bottom*). Data represent mean ± SEM; * $p < 0.05$ vs. control, † $p < 0.05$ vs. IGF-1 treated group.

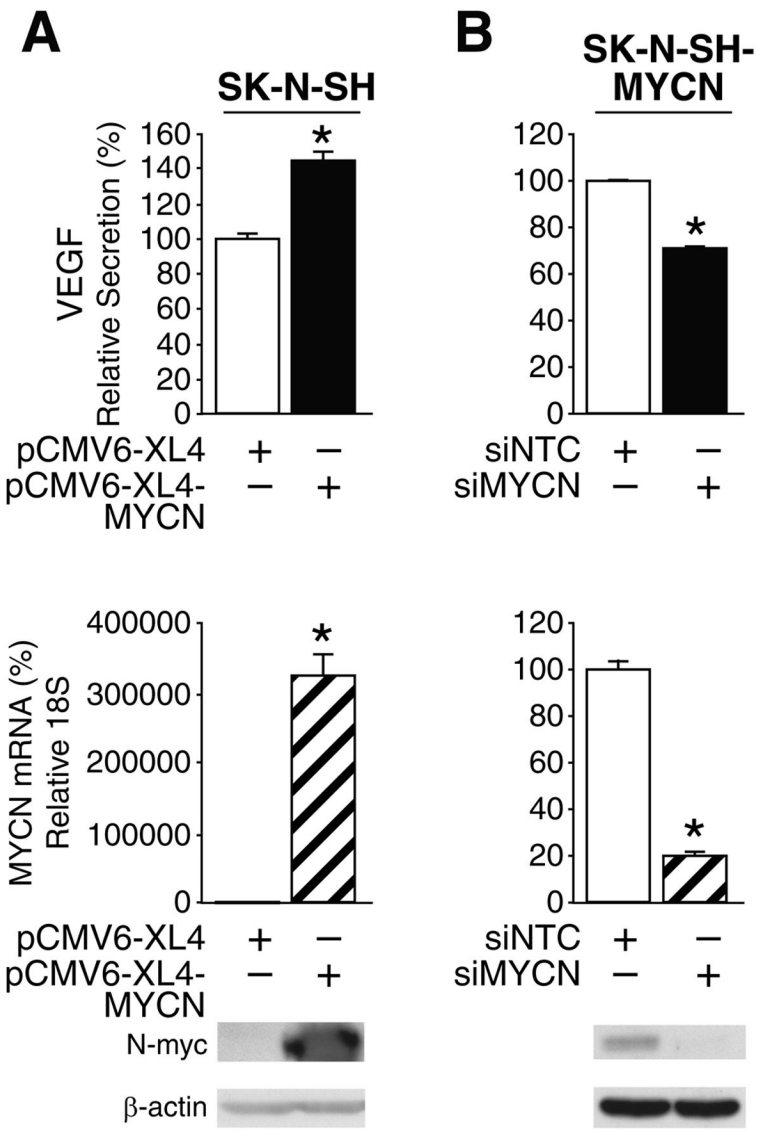

Figure 5. *MYCN* overexpression stimulates VEGF secretion

A. *MYCN* non-amplified SK-N-SH cells were transfected with *MYCN* vector and VEGF secretion was assessed (*top*). N-myc expression was determined by QRT-PCR and Western blot analysis (*bottom*). Data represent mean ± SEM; * $p < 0.05$ vs. control vector. **B.** SK-N-SH cells expressing *MYCN* vector were transfected with siMYCN; VEGF secretion was assessed (*top*). N-myc expression was determined by QRT-PCR and Western blot analysis (*bottom*). Data represent mean ± SEM; * $p < 0.05$ vs. siNTC.

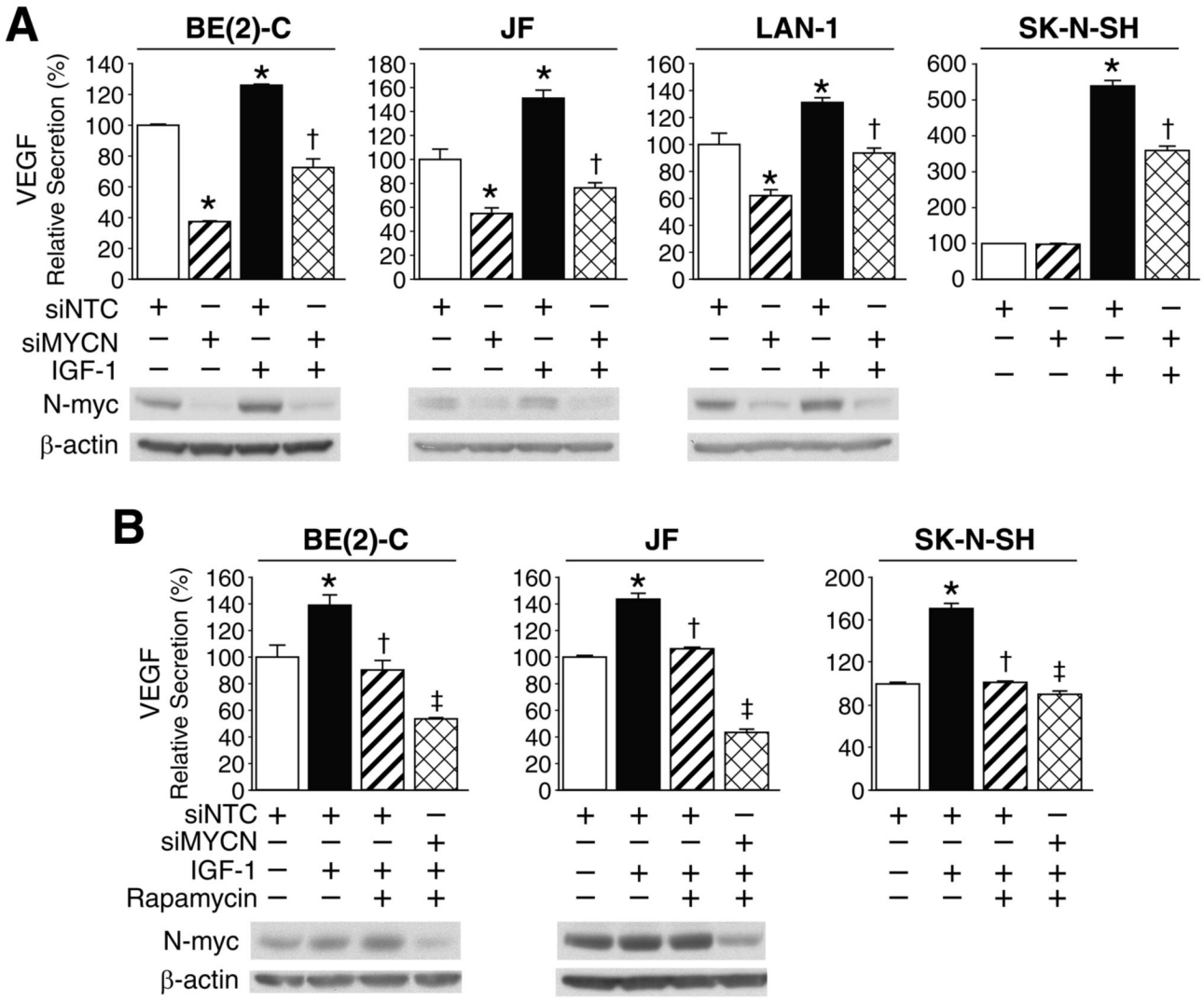

Figure 6. *MYCN* silencing attenuates VEGF and enhances rapamycin-mediated inhibition of VEGF secretion

A. BE(2)-C, JF, LAN-1 and SK-N-SH cells were transfected with siMYCN or siNTC overnight and serum-starved for 24 h. IGF-1 was added with fresh serum-free medium for 16 h. Conditioned medium was analyzed for VEGF secretion (*top*). Protein lysates were probed with N-myc antibody (*bottom*). **B.** BE(2)-C, JF and SK-N-SH cells were transfected with siMYCN or siNTC in the absence or presence of rapamycin and/or IGF-1, and medium was analyzed for VEGF secretion (*top*). Protein lysates were probed with N-myc antibody (*bottom*). Data represent mean ± SEM; * $p < 0.05$ vs. control group, † $p < 0.05$ vs. IGF-1 treated group, and ‡ $p < 0.05$ vs. IGF-1 and rapamycin treated group.

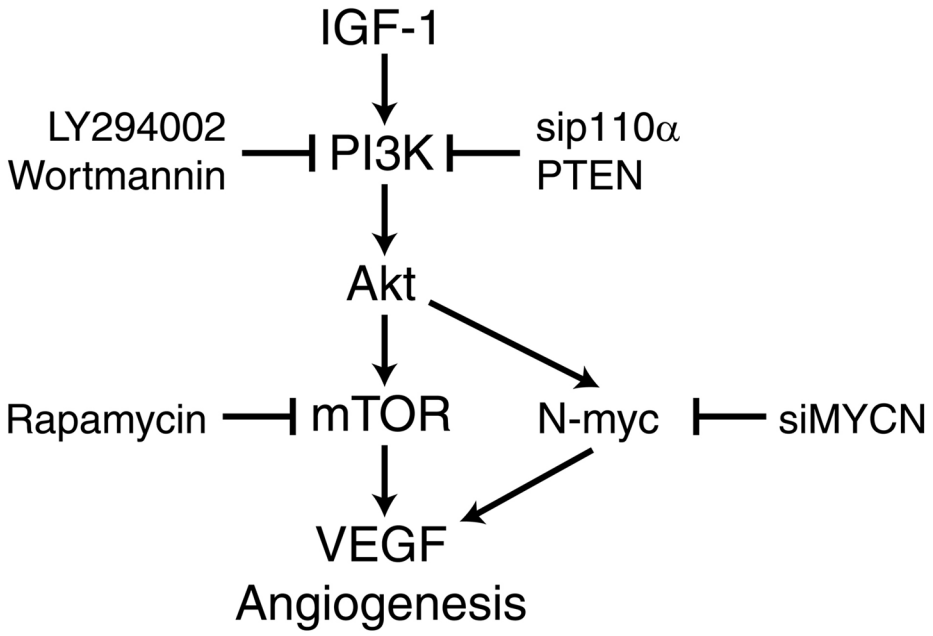

Figure 7.
Proposed mechanism of PI3K and N-myc regulation of VEGF/angiogenesis.